Ecological Modelling 356 (2017) 38–47

Contents lists available at ScienceDirect

Ecological Modelling

journal homepage: www.elsevier.com/locate/ecolmodel

Marine phytoplankton biomass responses to typhoon events in the South China Sea based on physical-biogeochemical model

Gang Pan[a,*], Fei Chai[b], DanLing Tang[a], Dongxiao Wang[a,*]

[a] State Key Laboratory of Tropical Oceanography (LTO), South China Sea Institute of Oceanology, Chinese Academy of Sciences, Guangzhou, 510301, China
[b] School of Marine Sciences, University of Maine, Orono, ME 04469, USA

ARTICLE INFO

Article history:
Received 3 November 2016
Received in revised form 3 March 2017
Accepted 21 April 2017

Keywords:
Typhoon
Phytoplankton bloom
Primary productivity
South China sea
ROMS-CoSiNE model

ABSTRACT

Most previous studies confirmed that marine phytoplankton biomass can increased dramatically and then formed blooms along the typhoon track after typhoon passage. However, many events of no significant responses to typhoons were neglected. In order to figure out the most important factor for bloom formation, a coupled physical-biogeochemical model was used to study the biogeochemical phytoplankton responses to all 79 typhoon events that affected the South China Sea (SCS) during 2000–2009. The major factors investigated included typhoon intensity and translation speed, Chlorophyll a concentration (Chl-a) and vertical nitrate transport in the euphotic zone before and after typhoon passage. The results revealed that phytoplankton blooms were triggered after 43 typhoon events, but no significant blooms were found after 36 other typhoons. Of the 43 typhoon events that triggered blooms, 24 were in the open ocean and 19 were on the coast. Subsurface blooms were detected after five typhoon events that did not trigger surface blooms. Over half of the typhoons that affect the oligotrophic SCS can trigger phytoplankton blooms, and contribute to the marine primary productivity. The mechanism of the above results were surveyed, we found that (1) an increased nitrate concentration is the basic and key precondition for phytoplankton blooming in the oligotrophic SCS; (2) typhoon intensity, and translation speed control the upward flux of nitrates together, and translation speed has more effect than intensity; (3) uplifted nitrates could trigger phytoplankton bloom, and Chl-a levels reached a peak 3 days later than nitrate levels; (4) mesoscale eddies and the nutricline depth before a typhoon's arrival also affects bloom genesis; and (5) the composition of phytoplankton functional groups in the coast was adjusted by typhoon, which have more complex mechanism of bloom formation than that in the open ocean. In summary, the physical driving force that modulates blooms is vertical nutrient transportation in the SCS.

1. Introduction

Typhoons (also referred to as tropical cyclones, or hurricanes) are powerful sea surface dynamical processes that are generated in tropical oceans. It is well known that the vertical mixing and upwelling induced by typhoons can uplift the deeper chlorophyll to the surface, and bring nutrient-rich deeper water up into the upper euphotic zone (Price, 1981; Shang et al., 2008; Zheng and Tang, 2007). The uplifted nutrients can trigger phytoplankton blooms (as measured by Chlorophyll a concentration, Chl-a) and increase marine new productivity, particularly in oligotrophic tropical oceans (Lin et al., 2003; Shang et al., 2008; Ye et al., 2013; Zhao et al., 2008). Most previous studies on biogeochemical phytoplankton responses to typhoons focused on positive event, in which obvious phytoplankton blooms were observed by satellite remote sensing (Babin et al., 2004; Lin, 2012; Subrahmanyam et al., 2002; Walker et al., 2005) and field observation (Naik et al., 2008; Shiah et al., 2000; Zhang et al., 2014). There are separate typhoon events, case by case. Many events of no significant responses to typhoons were neglected. Lin (2012) systematically checked phytoplankton blooms induced by all 11 typhoon events in the part of pacific ocean (15–25°N, 127–180°E) in 2003, and found that only two (18%) phytoplankton blooms occurred (Lin, 2012).

The South China Sea (SCS) is the largest marginal ocean of the pacific ocean, and a third of the typhoons generated in the North-West Pacific Ocean (NWPO) affect the SCS, with about 8 typhoons per year (Mendelsohn et al., 2012; Wang et al., 2007; Zhao et al., 2008) (Fig. 1). Typhoon plays an important role in enhancing phytoplankton biomass and primary productivity in oligotrophic SCS (Lin et al., 2003; Shang et al., 2008; Zhao et al., 2008; Zheng and Tang,

* Corresponding authors.
E-mail addresses: gpan@scsio.ac.cn (G. Pan), dxwang@scsio.ac.cn (D. Wang).

http://dx.doi.org/10.1016/j.ecolmodel.2017.04.013
0304-3800/

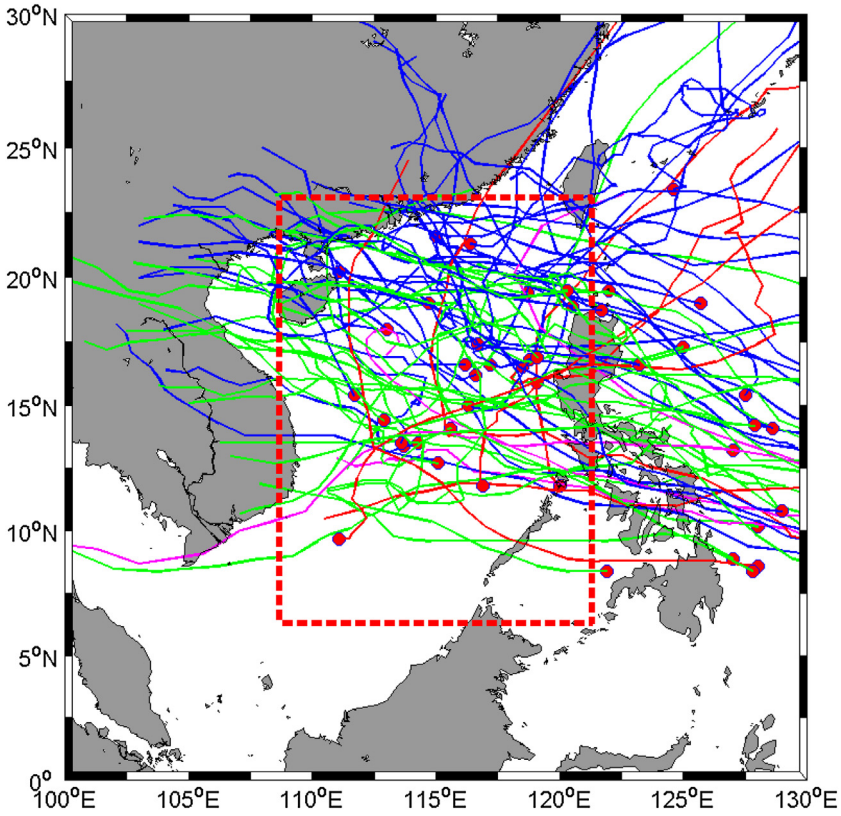

Fig. 1. Tracks of typhoon observed between 2000 and 2009, which affected the South China Sea and adjacent ocean. Red dashed box (6°–24°N, 108°–122°E) indicates the study area. Red solid circles present the place of typhoon genesis; red, blue, green, and magenta lines are typhoon tracks in spring (MAM), summer (JJA), autumn (SON), and winter (DJF), respectively. Gray patch means land. (For interpretation of the references to colour in this figure legend, the reader is referred to the web version of this article.)

2007). However, few phytoplankton blooms triggered by typhoon have been detected. The factor that is the most important for bloom formation is unknown. Checking the typhoon events systematically is a good method to figure out the key factor.

In general, marine phytoplankton blooms along the typhoon's track after its passage can be observed by satellite remote sensing (Babin et al., 2004; Lin, 2012; Subrahmanyam et al., 2002; Walker et al., 2005) and field observations (Naik et al., 2008; Shiah et al., 2000; Zhang et al., 2014). However, visible/infrared satellite sensors [i.e., Sea-Viewing Wide Field-of-View Sensor (SeaWiFS) and Moderate Resolution Imaging Spectroradiometer (MODIS)] are sensitive to cloud cover; therefore, they do not provide a clear spatial or temporal indication of typhoon-induced responses. Field observations of pre- and post-typhoon phytoplankton biomasses are few, because of the dangers inherent in fieldwork associated with typhoon events. Therefore, a reliable technique is needed.

Physical-biogeochemical models that link physics and ecosystem components with phytoplankton growth are useful tools with which to fill the gaps in space and time in field and satellite observations. Therefore, physical-biogeochemical models, once their performance has been evaluated by available observations, provide an alternative means of investigating the overall response of the upper ocean to typhoons (Chai et al., 2009; Gierach et al., 2009; Hung et al., 2010; Shibano et al., 2011). However, only a few individual typhoons' passages have been investigated in terms of Chl-a and nutrient responses by combining biogeochemical processes with physical models, such as Katrina in 2005 in the Gulf of Mexico (Gierach et al., 2009), and Keith in 1997 in the NWPO (Shibano et al., 2011).

Until now, to our knowledge, the contributions of all typhoon events over several years have never been systematically quantified. The purpose of this study was to simulate phytoplankton and nutrient responses to typhoon events, characterize blooms after a typhoon's passage, determine the factors that affect bloom genesis, and elucidate the mechanisms involved. A coupled three-dimensional physical-biogeochemical model (i.e. the Regional Ocean Modeling System (ROMS)–Carbon, Si(OH)$_4$, Nitrogen Ecosystem (CoSiNE) model, ROMS–CoSiNE model) was used.

2. Methods

2.1. Study area

The SCS has a total area of about 3.5 million km^2. Its bottom topography is characterized by a basin with a maximum depth of 5000 m at the center, wide continental shelves in the north and south, and steep slopes in the east and west (Chai et al., 2009; Tang et al., 2004). It has tropical oligotrophic surface waters, with a shallow mixed layer and nutricline depths (Gong et al., 1992; Wang et al., 2012; Wong et al., 2007). The NWPO has the highest density of typhoons in the world, both in number and intensity (Mendelsohn et al., 2012; Wang et al., 2007).

The distribution of small phytoplankton (<5 μm in diameter) in the SCS is highly uniform. The annual mean depth-integrated phytoplankton concentration in the entire basin is estimated to be ~35 mmol m^{-2}. Diatoms mainly exist in the central and southern basins, and high concentrations are found from western Luzon Island to eastern Vietnam. The annual average total phytoplanktonic carbon content is similar to that of diatoms, i.e., diatoms account for the majority of the biomass (Ma et al., 2013). The main

Table 1
Summary of phytoplankton blooms were observed using satellite remote sensing after typhoon passage.

		before		after		
typhoon name	area	phyto (mg m^{-3})	data	bloom (mg m^{-3})	data	references
Ivan	GoM	0.36	mean 4d	0.81	day	Walker et al. (2005)
	GoM	0.24	mean 4d	0.99	day	
Ling-ling 2001	SCS	0.14	climatologies	0.54	mean 8d	Zhao et al. (2008)
Kai-tak 2005	SCS	0.15	climatologies	0.45 (max 1.05)	mean 8d	
Kai-tak 2000	SCS	0.1	mean 8d	0.56 (max 3.2)	mean 4d	Lin et al. (2003)
Ling-ling 2001	SCS	0.08	mean 5d	0.37	day	Shang et al. (2008)
Damrey 2005	SCS	0.129	mean 2d	>1 (max 4.1)	day	Zheng and Tang (2007)
Katrina 2005	GoM	0.2	8d L3	0.53 (peak 2.69)	day	Gierach and
Rita 2005	GoM	0.2	8d L3	(peak 1.97)	day	Subrahmanyam (2008)
Nakri 2008	NWP	0.05	8d	0.3		Zheng et al. (2010)
08A 1998	Arabian S	0.4	weakly	>1 (max 4)	weak	Naik et al. (2008)
Fengwong 2008	ECS	0.77	mean 3d	0.93	mean 3d	Hong et al. (2010)
Sinlaku 2008	ECS	0.3	mean 3d	0.7	mean 3d	
Hagibis 2007	SCS	0.1–0.2	mean 20d	5	weak	Sun et al. (2010)

limitation to phytoplankton growth is the availability of nutrients (Chen et al., 2004; Tang et al., 2004; Wang et al., 2012).

2.2. ROMS–CoSiNE coupled model

We coupled the ROMS with the CoSiNE model to investigate changes in Chl-a and nitrate levels before and after typhoon events. ROMS is a physical ocean model widely used by the scientific community (Shchepetkin and McWilliams, 2005). This ROMS model domain is for the entire Pacific Ocean (45°S–65°N, 99°E–70°W). The horizontal grid size is 1/8°, and there are 30 terrain-following levels in the vertical direction (Wang and Chao, 2004). In this study, we only used model outputs for the SCS domain (5°S–25°N, 100°E–125°E; the model resolution is about 12.5 km in the SCS). The CoSiNE model is developed by (Chai et al., 2002; Dugdale et al., 2002). The CoSiNE model has ten components representing two sizes of phytoplankton, small phytoplankton cells (S1) (<5 mm in diameter) and diatoms (S2), micro- and meso-zooplankton (Z1 and Z2), non-living detrital nitrogen and silicate, dissolved silicic acid, and two forms of dissolved inorganic nitrogen: nitrate and ammonium, total CO_2. S1 represents small, easily grazed phytoplankton whose specific growth varies, but whose biomass is regulated by micrograzers (Z1). S2 represents relatively large phytoplankton (>5 mm in diameter) that makes up high biomass blooms. The S2 phytoplankton class has the potential to grow fast under optimal nutrient conditions. The detrital pool is split into detrital nitrogen and silicon in order to balance supplies of nitrogen and silicon through the upwelling and vertical mixing separately. The pacific version of the ROMS-CoSiNE used here was forced with satellite-derived blended-wind stress and National Centers for Environmental Prediction (NCEP) heat and freshwater fluxes. Model results are compared with field data for new and total nitrogen production and export of N, Si, and C, that match very well with the Joint Global Ocean Flux Study (JGOFS) data. More detailed descriptions of the coupled model are given in (Xiu and Chai, 2011, 2012) The nominal temporal resolution of the three-dimensional variables was 73 h (3 days and 1 h), and each time slice represented the values of the biogeochemical variables averaged over the 73 h period.

The CoSiNE model was forced by the upwelling velocity and vertical diffusivity obtained from the pacific version ROMS model, which had been compared with the satellite data in the SCS and the Gulf of Alaska (Xiu et al., 2010, 2012). The coupled ROMS-CoSiNE model can reproduce the general features of the ocean dynamics in the pacific ocean, such as nutrient transport, phytoplankton biomass, phytoplankton functional groups, and new production, which are in agreement with the in situ observation in the South East Asia Time-Series Station (SEATS) station (18°N, 116°E) and some research cruises in the SCS and the Sea of Japan (Chai et al., 2009; Liu and Chai, 2009; Ma et al., 2013; Xiu and Chai, 2011); and the CoSiNE simulated nitrogen uptake rates and phytoplankton community composition are validated by the data from the two research cruises undertaken in December 2004 and September 2005 in the equatorial upwelling zone in the pacific ocean (Alexander et al., 2008; Chai et al., 2007; Parker et al., 2011); the phytoplankton, zooplankton, and SST derived from the pacific version ROMS-CoSiNE model were calibrated by satellite data and field campaign observation in the Peru upwelling area (Xu et al., 2013). According to abovementioned, the use of the coupled model could significantly advance our understanding of the biogeochemical responses to typhoon passage in the SCS.

2.3. Typhoon track data

The typhoon track data used in this study were downloaded from the webpage of the National Institute of Informatics of Japan (http://agora.ex.nii.ac.jp/digital-typhoon/search_date.html.en), and were based on the best typhoon track data issued by the Joint Typhoon Warning Center. The track data included typhoon location and intensity (maximum sustained winds in knots, and central atmospheric pressure in mbar) every 6 h.

The typhoon dataset covers the period 2000–2009. We chose all typhoon events that had an impact on the SCS, including typhoons in the area of 6–24°N and 108–122°E (Fig. 1).

2.4. Phytoplankton bloom criteria

The average Chl-a level between 5 and 12 days before typhoon arrival was considered the background value (Table 1), and the difference in Chl-a levels between after the typhoon's passage and the background value was used to identify blooms, which were identified using satellite remote sensing (Babin et al., 2004; Lin, 2012; Subrahmanyam et al., 2002; Walker et al., 2005) and field observations (Naik et al., 2008; Shiah et al., 2000; Zhang et al., 2014). Blooms last for about 1–2 weeks and then disappear. In this study, we selected simulated model outputs that had been averaged over 2–4 time slices (corresponding to 5–13 days) before typhoon arrival as background values, because each time slice model output represented the variables averaged over a 3 day period. The change in Chl-a (ΔC) was the difference between the Chl-a level after the typhoon's passage and the background value. Areas in which $\Delta C > 0.5$ mg m^{-3} and that were 200 km or closer to the typhoon's track were identified as bloom areas (Fig. 2).

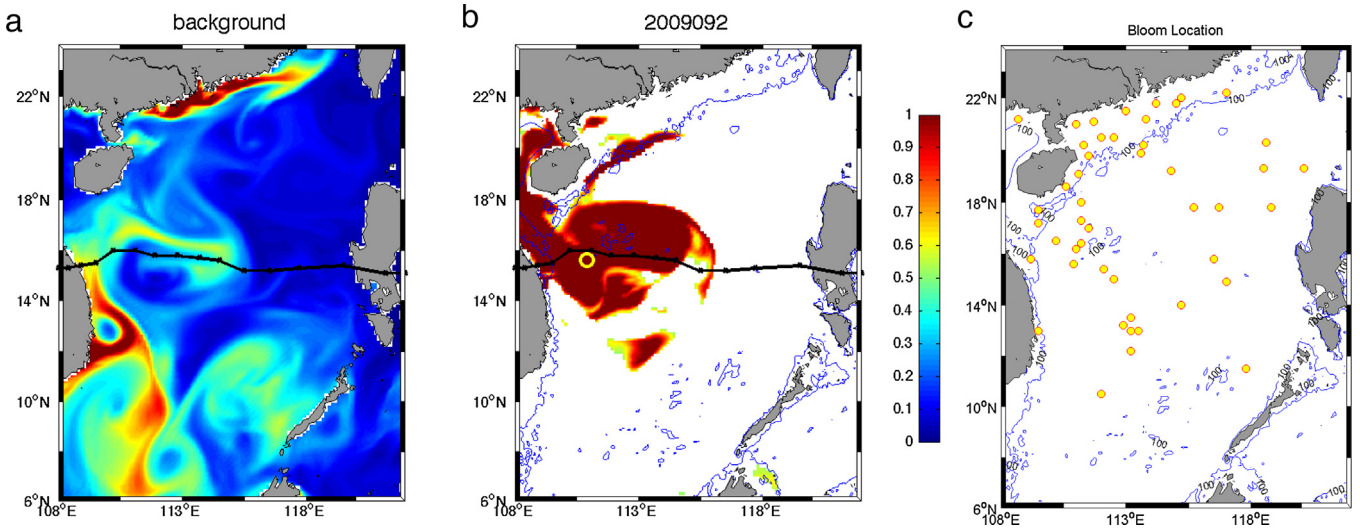

Fig. 2. A phytoplankton bloom was defined. The averaged Chl-a between 5 and 13 days before typhoon Ketsana (200916) arrival was considering as background value (a), the difference of Chl-a after the typhoon passage and the background (b) was used to identify the bloom. All 43 blooms were identified in (c), 24 of them in open ocean, and 19 in coastal. The colorbar shows the Chl-a concentration (mg m^{-3}). Black thick line represents the typhoon track; yellow circle means the location of bloom, and blue line means 100 m isobaths. (For interpretation of the references to colour in this figure legend, the reader is referred to the web version of this article.)

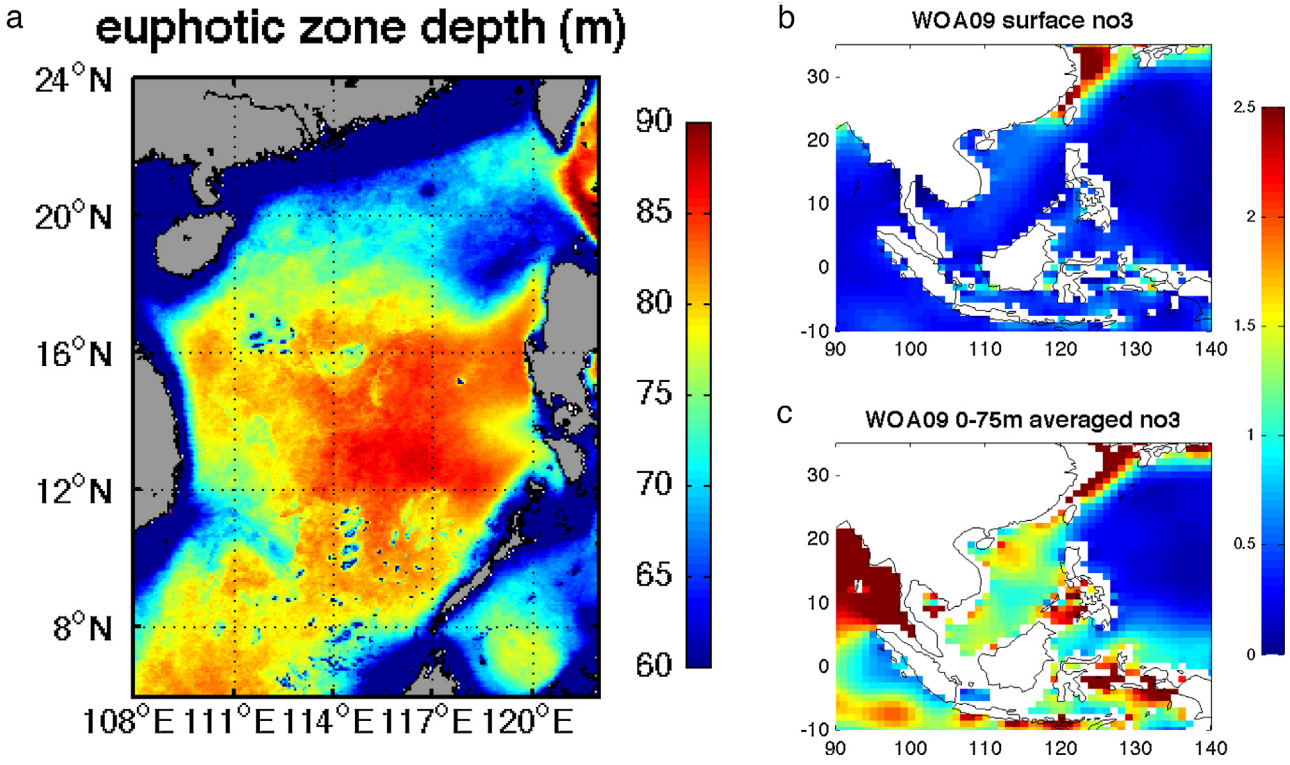

Fig. 3. Climatological euphotic zone depth (a), surface nitrate (b) and 0–75 m averaged nitrates (c) in SCS. According to the approach of Morel et al. (2007), euphotic zone depth was derived from the entire mission composite (Jul 2002–Apr 2014) 4 km resolution Aqua MODIS chlorophyll concentration data. The averaged depth was 71.5 m in the study area. Seasonal depth was 77, 75, 69, 65 m in spring, summer, autumn, and winter, respectively.
Zeu was derived by:
$\log10(Zeu) = 1.524 - 0.436X - 0.0145X\hat{2} + 0.0186\ X\hat{3}$
with $X = \log10(Chl\text{-}a)$.
Nitrate concentration obtained from World Ocean Atlas 2009 (WOA09).

The modeled Chl-a level was derived from the phytoplankton biomass concentration (mmol N m^{-3}), and was converted to mg m^{-3} using a nominal gram chlorophyll-to-molar nitrogen ratio of 1.67, which corresponded to a chlorophyll-to-carbon mass ratio of 1/50 and a C/N molar ratio of 7.3 (Chai et al., 2009). To investigate the mechanisms involved in the formation and dispersal of phytoplankton blooms, Chl-a and nitrate levels, which were averaged from the surface to the euphotic layer, were simulated. We averaged nitrate and Chl-a levels from 0 to 75 m, which is close to the bottom of the euphotic zone in the SCS (Morel et al., 2007) (Fig. 3a).

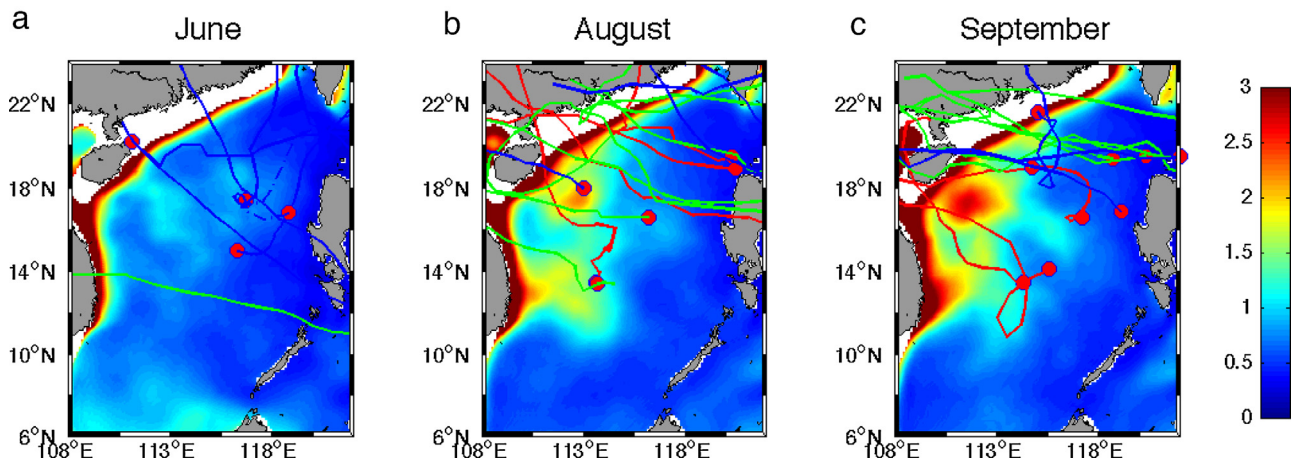

Fig. 4. Typhoon tracks in different months. The background color shows the model simulated monthly 0–75 m averaged NO_3 concentration in Jun (a), Aug (b), and Sep (c) during 2000–2009. Typhoon track was superimposed. Red solid circles present the place of typhoon genesis, and red, green, blue lines present typhoon tracks, which can trigger bloom in open sea (red), coastal (green), and no surface bloom (blue), respectively. (For interpretation of the references to colour in this figure legend, the reader is referred to the web version of this article.)

3. Results

3.1. Model driver and its validation

We followed the approach of Wang and Chao (2004) for setting up the ROMS model, but increase the horizontal resolution to 12.5 km for the entire Pacific Ocean domain. Initialized with climatological temperature and salinity from the World Ocean Atlas 2001, the Pacific ROMS model has been forced with the climatological NCEP/NCAR reanalysis of air-sea fluxes (Kalnay et al., 1996) for several decades in order to reach quasi-equilibrium. The model is then integrated for the period of 1991–2010 forced with daily air-sea fluxes of heat and freshwater from the NCEP reanalysis (Kalnay et al., 1996). The typhoon wind and pressure fields were estimated using the observed typhoon track and central pressure.

The ROMS-CoSiNE model can simulate the characteristics of biogeochemical variables in a way that is comparable with field and satellite observations. The modeled eddy kinetic energy, eddy number, and eddy-occupied area agreed well with results from Archiving, Validation and Interpretation of Satellite Oceanographic (AVISO) data (Xiu et al., 2010, 2012); the modeled Chl-a and particulate organic carbon levels showed a high correlation with SeaWiFS satellite derivations ($R = 0.8$, $p < 0.01$) (Ma et al., 2013; Xiu and Chai, 2011) in reproducing Chl-a, nitrate, silicate, and total CO_2 level and their variability over the same period, which were obtained from the SEATS station (18°N, 116°E) and some research cruises in the SCS (Chai et al., 2009; Liu and Chai, 2009).

3.2. Effect of typhoon diversity on blooms

There were 79 typhoon events in the SCS during 2000–2009, and 53% of them occurred in July, August, or September. Over the same period, there were 239 typhoon events in the whole NWPO. Of the 79 typhoon events in the SCS, 50 were generated in the NWPO and moved to the SCS, and nine were generated in the SCS and moved to the NWPO. Twenty typhoon events were confined to the SCS (Fig. 1). In general, the number of typhoon events slightly increased over the 10-year period, as did the number of typhoon events globally.

Blooms were detected after 43 typhoon events, but no significant blooms were found after 36 other typhoons. Of the 43 typhoons that triggered blooms, 24 were over the open ocean (deeper than 100 m) and 19 occurred in coastal areas (shallower than 100 m) (Fig. 2). Subsurface blooms were detected after five typhoon events without surface blooms.

Table 2
Statistics analysis of typhoon intensity and translation speed in different months.

month	type	intensity (mb)	intensity (kt)	speed (m/s)
June	coastal	975	60	6.7
	no bloom	971.6 ± 16.8	63.6 ± 17.0	4.3 ± 1.7
	month	972.0 ± 15.6	63.1 ± 15.8	4.6 ± 1.8
August	deep sea	977.5 ± 6.5	52.5 ± 10.4	2.8 ± 1.2
	coastal	982.9 ± 15.1	49.2 ± 16.9	5.0 ± 1.1
	no bloom	981.0 ± 14.6	51.3 ± 16.5	4.5 ± 1.1
	month	980.9 ± 12.5	50.7 ± 14.1	4.3 ± 1.4
September	deep sea	981.0 ± 22.9	51.7 ± 20.2	4.3 ± 1.8
	coastal	967.5 ± 20.1	65.0 ± 20.7	5.1 ± 3.0
	no bloom	989.7 ± 4.5	38.3 ± 2.9	5.3 ± 1.8
	month	976.4 ± 19.5	55.0 ± 20.1	4.9 ± 2.3

3.3. Effect of typhoons in different months

Of the 79 typhoon events, 15 and 12 occurred in August (Fig. 4b) and September (Fig. 4c), respectively. These two months had the highest frequency of typhoons. Furthermore, 20 of 27 events (74%) triggered phytoplankton blooms. We simulated the average monthly surface and 0–75 m depth nitrate levels in the different months from 2000 to 2009 (Fig. 4). According to the simulated nitrate profiles, there is a shallower nutricline during these months. Typhoons cause seawater containing high concentrations of nitrate to rise to the euphotic zone, which induces phytoplankton blooms.

There were eight typhoons in the SCS in June (Fig. 4a). Only one (12.5%) (Chanthu, ID 200405) triggered a phytoplankton bloom, which appeared in the west of the SCS, where the nitrate level was much higher than in the surrounding waters (Fig. 4a). No surface phytoplankton blooms were found after the other seven typhoons. According to the simulated nitrate profile, there are lower average surface and 0–75 m depth nitrate levels in June. A subsurface bloom was found after typhoon Chan-Hom (ID 200902), but no significant surface bloom was observed.

Typhoons in June have a lower central atmospheric pressure and a higher maximum sustained wind speed than those in August or September (Table 2). Typhoon translation speed is similar in different months. The statistical analysis revealed that few phytoplankton blooms appear after typhoons in June. In contrast to typhoons in August and September, those in June have a stronger intensity, and consequently are stronger driving forces for nutrient transportation. However, because of the deeper nutricline, the strong driving force cannot uplift a sufficient amount of nitrates

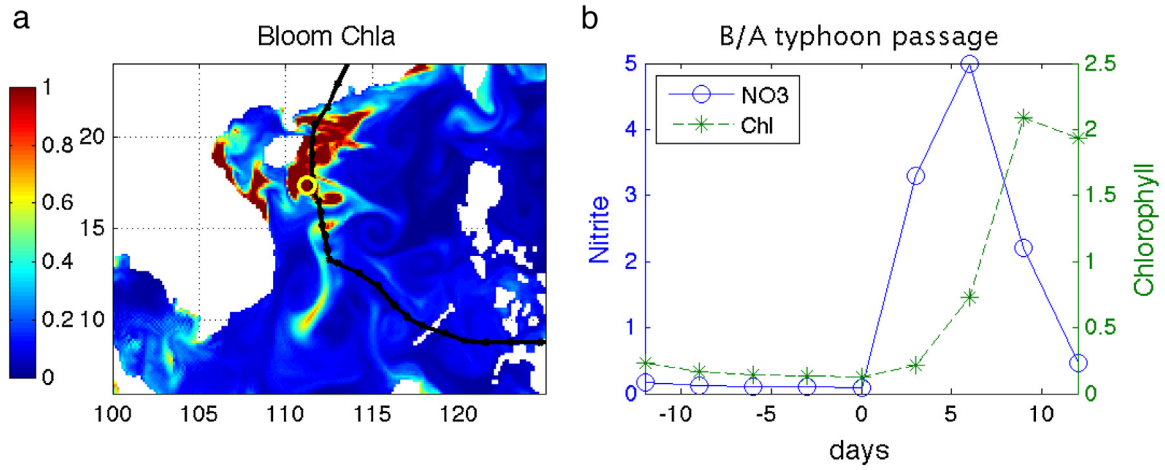

Fig. 5. Chl-a (*) and NO_3 (o) concentration at before and after typhoon Neoguri (200801) passage (b). The concentration was averaged using 5 by 5 pixels, and the central of 5 by 5 box is the location of bloom, which was shown as yellow circle in (a). The background color refers to the Chl-a concentration during the bloom. (For interpretation of the references to colour in this figure legend, the reader is referred to the web version of this article.)

to the eutrophic zone to trigger a phytoplankton bloom (Fig. 4a); consequently, fewer are triggered by typhoons in June.

3.4. Effect of nutrient concentration on bloom genesis

As oceans are highly spatially heterogeneous, we used averaged 5×5 pixel model outputs to investigate the temporal variability of nitrate and Chl-a levels in bloom areas, both before and after the typhoon's passage. Before typhoon arrival, Chl-a levels are generally low with values lower than 0.2 mg m^{-3} in most of the study area. In the case of typhoon Neoguri (ID 200801), the surface nitrate level dramatically increased from 0.13 mmol N m^{-3} before the typhoon to 3.30 mmol N m^{-3} after, and reached a peak of 4.99 mmol N m^{-3}. The Chl-a level increased from 0.18 to 0.22 mg m^{-3}, and then to 0.73 mg m^{-3}, and reached a peak of 2.09 mg m^{-3}. The Chl-a peak was 3 days later than the nitrate peak (Fig. 5). In the case of typhoon Ketsana (ID 200916), a large area of seawater with high nitrate concentrations appeared along the typhoon's track after its passage.

Regarding the average surface (Fig. 6a) and 0–75 m depth (Fig. 6c) nitrate levels, we found that surface nitrate levels are lower than those deeper. Deep high-nitrate-containing seawater is uplifted to the eutrophic zone. The nitrate transportation process is shown in Fig. 7. In the eutrophic zone (0–75m), there are low nitrate levels in the 15.6°N section before the typhoon's arrival (Fig. 7a), and high levels after its passage (Fig. 7b). The nitrate profile in the bloom area during typhoon events (about 27 days) is shown in Fig. 7c. Before the typhoon's arrival, the nitrate level in the eutrophic zone is low; with its arrival, nitrate levels in the eutrophic zone increase sharply, before gradually decreasing. After the nitrate is uplifted to the eutrophic zone, large, high Chl-a content areas of seawater are found in the same places along the typhoon's track (Fig. 6b), indicating that phytoplankton are utilizing the uplifted nitrates.

A comparison of the nitrate and Chl-a levels before and after a typhoon's passage revealed several patterns. Firstly, before the typhoon's arrival, surface Chl-a and nitrate level in the euphotic zone are very low in the oligotrophic SCS. Secondly, during the typhoon's passage and over the following few days, nitrate and Chl-a levels increase sharply before gradually decreasing. Thirdly, Chl-a levels peak after those of nitrate have peaked. Changes in nitrate supply is a key factor in controlling the amount of phytoplankton biomass (Chl-a). Phytoplankton biomass gradually increases after the nitrate concentration in the euphotic zone increases, and then decreases to a low concentration once the nitrates have been consumed.

4. Discussion

4.1. Physical factors affect nitrate transportation

It has been known for decades that slow moving or strong typhoons can cause larger phytoplankton blooms in the upper ocean than fast moving or weak typhoons, due to the duration or the strength of the force applied (Gierach and Subrahmanyam, 2008; Lin, 2012; Zhao et al., 2008). Many studies reported that bloom was not found at the point where this typhoon had its maximum strength (Lin, 2012; Shibano et al., 2011). The effects of the passing typhoon could not completely explain why the phytoplankton bloom developed at this location.

In the present study, we compared typhoon intensity and translation in different months (Table 2). In August, typhoons can trigger open-ocean phytoplankton blooms, and have a slower average translation speed (2.8 ± 1.2 m s^{-1}) and lower central atmospheric pressure than in the other months. A relatively long lingering time extends the influence of the entrainment/upwelling and mixing induced by typhoons; as a result, the increase of in Chl-a levels in regions with the strongest typhoons [e.g., Prapiroon (ID 200606)] was not more obvious than that in the two high Chl-a patches (Kammuri, ID 200212; Kammuri, ID 200809) with relatively slow translation speed. For typhoons with similar intensities, a slower translation speed (i.e., longer lingering time) has a much longer effect on the upper oceans, possibly by increasing mixing and upwelling, which induces a greater injection of nutrients from the subsurface waters. Typhoons in September have similar effects as those in August. Weak, slow-moving typhoons, which occur more frequently than strong typhoons, may strongly impact tropical marine ecosystems.

Lin (2012) investigated all 11 typhoon events that passed through the part of pacific ocean in 2003. Only two induced phytoplankton blooms, and the most intense typhoon on earth in 2003 (Meami) did not (Lin, 2012). Sun et al. (2010) investigated 11 typhoon events in the middle of the SCS from 1997 to 2007. Only a weak typhoon (Hagibis in 2007) had a notable effect on Chl-

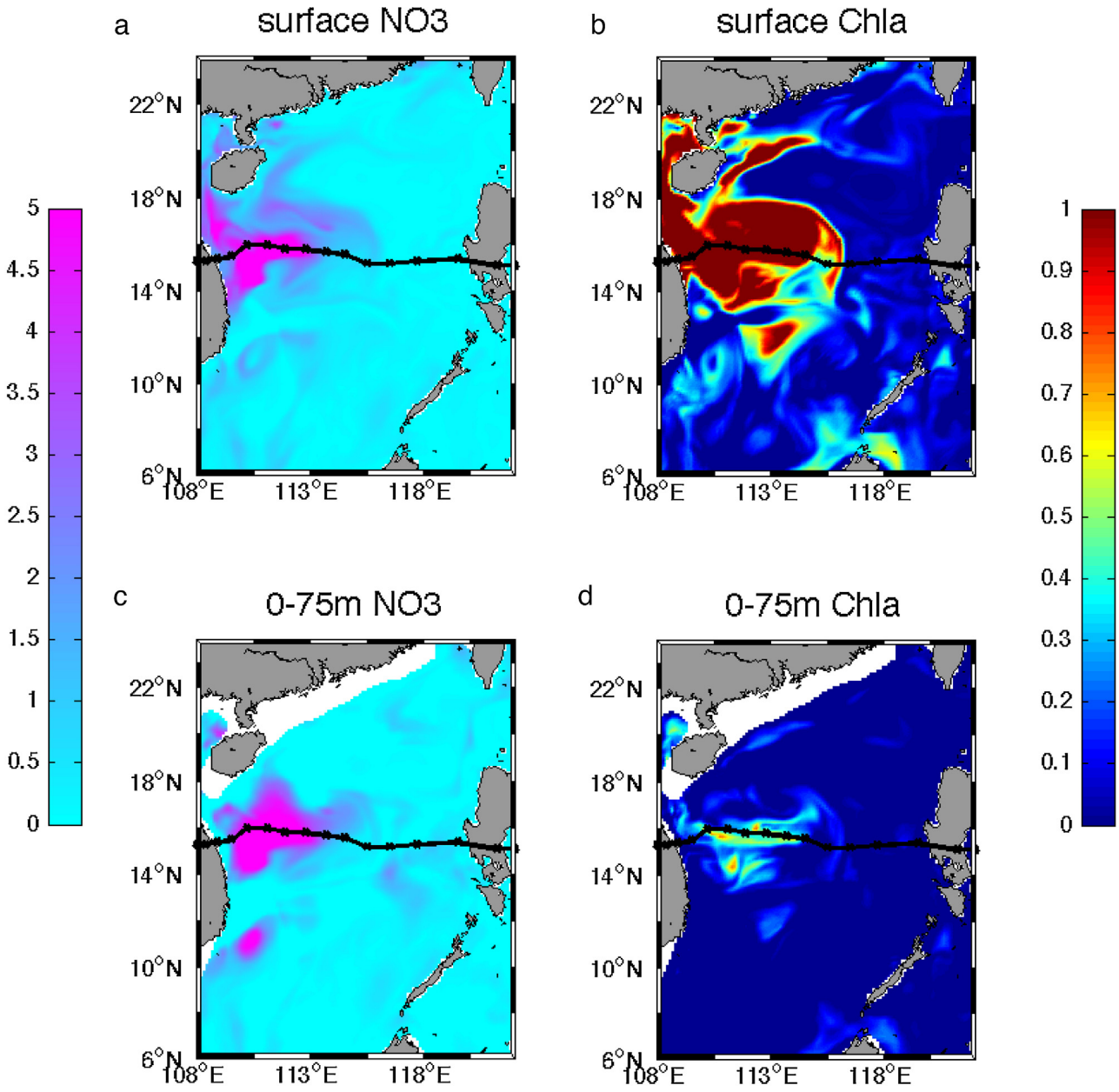

Fig. 6. Surface and 0–75 m averaged nitrate and Chl-a concentration after typhoon Ketsana (200916) passage. (a) and (c) were nitrate concentration 3 days after typhoon passage, and (b) and (d) were Chl-a concentration 6 days after typhoon passage. (a) and (b) were surface concentration, and (c) and (d) were 0–75 m averaged concentration. Black line shows the typhoon track.

a concentrations (Sun et al., 2010). In one typhoon event (Keith in 1997), no bloom occurred at the point where the typhoon had its maximum strength of 910 hPa on November 3 (Shibano et al., 2011). At the time of passage over the Gulf of Mexico, hurricane Katrina (2005) had a translation speed of 3.4 m s^{-1} and a minimum central pressure of 950 mbar. Gierach and Subrahmanyam (2008) suggested that the magnitude and orientation of the responses exhibited within the region of interest were the result of Katrina's slow translation speed, and not its intensity (Gierach and Subrahmanyam, 2008). These observations suggest that slow-moving typhoons have a stronger driving force than high-intensity ones due to strong wind stress that swirls the mixed layer (Price, 1981). Our results suggest that increases in surface nitrate and Chl-a levels strongly depend on translation speed. Typhoon lingering time seems to be as important as intensity, because the upwelling and mixing produced is maintained over a longer period.

4.2. Pre-existing oceanic condition

It is well known that phytoplankton blooms are caused by the vertical mixing and upwelling produced by slow-moving typhoons at the blooms' locations. However, it cannot be used to explain why and where blooms develop only according to the passing typhoon there is difficult to estimate where blooms develop according to the passing typhoon, and it remains unclear why some typhoons induced more extreme upper ocean responses in certain areas than in other areas along their tracks.

Observations and models both indicate that the background ocean environment, such as mesoscale eddies, ocean fronts, etc. could significantly modulate the upper ocean's dynamical and thermal responses to a typhoon. Jaimes and Shay (2009) showed that for similar wind speeds under hurricanes Katrina (2005) and Rita (2005), the mixed layer velocity was nearly twice high inside cold

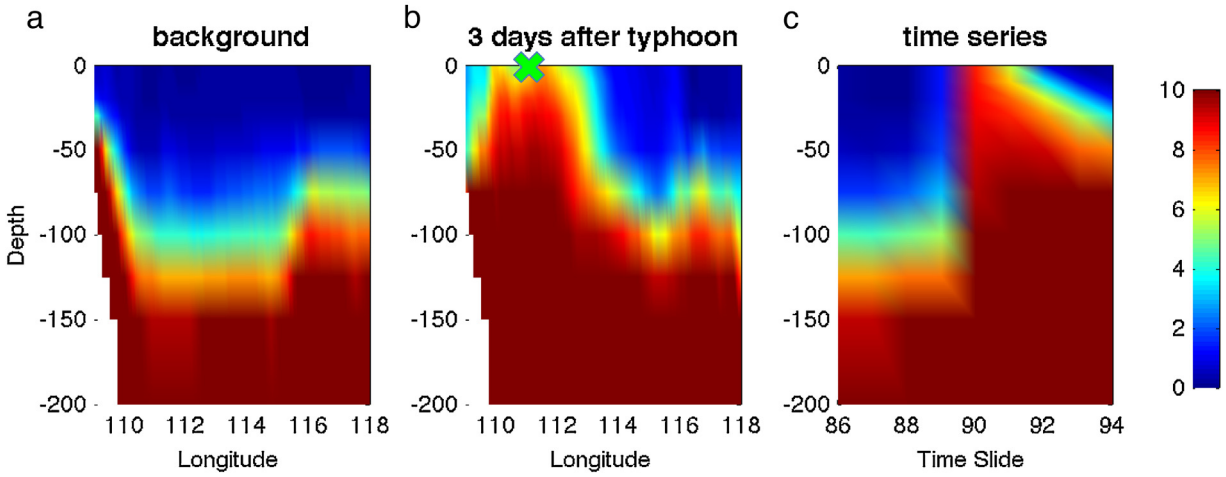

Fig. 7. 0–200 m vertical sections of nitrate at 15.6°N before (a) the typhoon Ketsana (200916) arrival and after (b) the typhoon passage. Identified bloom area (111.0°E, 15.6°N) was shown as green cross in Figure b, and nitrate evolutions associated with typhoon events were present in Figure c. The time series nitrate data were averaged using 5 by 5 pixels, which centered round the bloom area pixel. (For interpretation of the references to colour in this figure legend, the reader is referred to the web version of this article.)

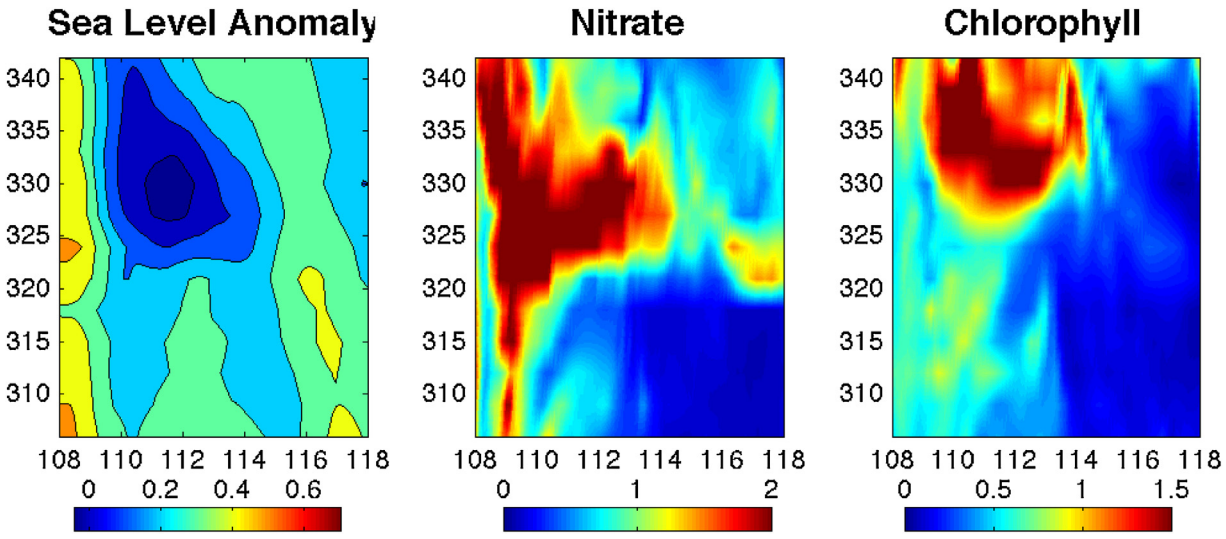

Fig. 8. Sea level anomaly, surface nitrate, and surface Chl-a evolution map before and after the typhoon Hagibis (200724). Horizontal axis means Longitude, and vertical axis means day of year. Typhoon Hagibis arrives in 10.5°N section on the 324th day of the year 2007.

core eddies as it was in warm core eddies, depending on the pre-hurricane ocean's mixed layer thickness (Jaimes and Shay, 2009). Walker et al. (2005) reported that hurricane-induced upwelling and increases in Chl-a concentration increased within cold-core typhoons in the Gulf of Mexico (Walker et al., 2005). Lin (2012) found that the presence of warm ocean eddies can effectively isolate cold, nutrient-rich water at the surface. In this situation, even Maemi (2003), a category five typhoon, could not induce phytoplankton blooms in the pacific ocean at its peak intensity of 150 knots (Lin, 2012). Our results are consistent with those from previous studies, suggesting a considerable effect of pre-existing cyclonic circulations on the strength of the upper ocean's responses to typhoons and the development of phytoplankton blooms. Before typhoon Hagibis's (ID 200724) arrival, eddies themselves did not generate a phytoplankton bloom at the surface, as can be seen in the Chl-a map (Fig. 8). One possible mechanism underlying phytoplankton blooms is that cold nutrient-rich water, which is normally in the nutricline depth of ~100 m (Gong et al., 1992), is brought up by eddies to the subsurface layer, but does not reach the surface layer because of strong stratification caused by warming. Indeed, it was the strong vertical mixing and upwelling induced by typhoon Hagibis that brought nutrients up to the surface, and thereby generated a phytoplankton bloom. Therefore, the upper ocean response is significantly related to the pre-existing background ocean features.

Nutricline depth is another important oceanic condition, and depends on the degree of water column stratification and the magnitude the momentum transfer associated with wind stress. (Gong et al., 1992) demonstrated that the nutricline in the SCS could be uplifted by as much as 100 m, and its surface water chlorophyll levels would be twice as high as under normal conditions. Under the strong wind stress caused by typhoons, deep, nutrient-rich seawater is uplifted to the surface. If the uplifted nutrients cannot reach the surface, a subsurface bloom may occur. Remote sensing observations have only provided measurements of the ocean's surface properties, such as the sea surface temperature and chlorophyll level, and have not provided any information from below the surface. Subsurface blooms are difficult to identify using traditional satellite remote sensing techniques, but are occasionally seen by ships (Ye et al., 2013). A subsurface bloom was seen after typhoon Chan-Hom (ID 200902), which did not trigger a significant sur-

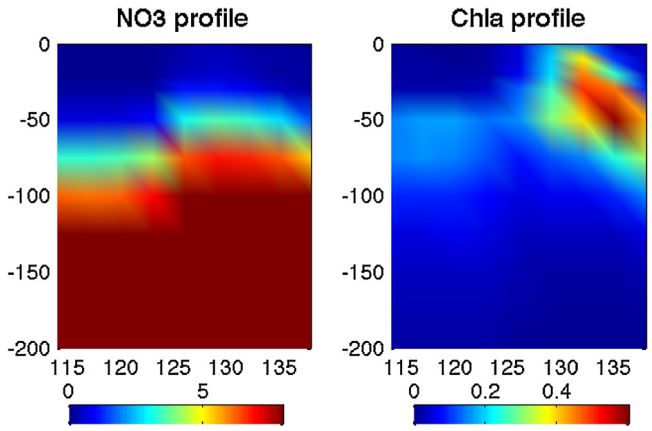

Fig. 9. Nitrate and Chl-a vertical profile (113°E, 13.2°N) evolution map before and after the typhoon Chan-Hom (200902). Horizontal axis means day of year, and vertical axis means depth. Typhoon Chan-Hom arrives in subsurface location on the 126th day of the year 2009.

face bloom. According to the nitrate profile, typhoon Chan-Hom increased the nitrate concentration to 6 mmol N m^{-3} at approximately the 50 m isobaths (Fig. 9), and only a subsurface bloom was triggered.

4.3. Differences between the coastal and open ocean

Of the 43 typhoon events that triggered blooms, 24 were in the open ocean and 19 were on the coast. The strong winds that are associated with typhoons can cause vertical entrainment and upwelling, which bring up nutrients from deeper layers to the upper euphotic zone, and produce phytoplankton blooms. This is how blooms form in the open ocean. On the coast, however, entrainment and upwelling can also result in sediment re-suspension and transport from nearby locations, and hurricane-induced sediment re-suspension in the eastern Gulf of Mexico has been reported (Chen et al., 2007). Shang et al. (2008) investigated the bloom triggered by typhoon Ling-Ling (ID 200123), and stated that dissolved organic matter and detritus significantly affected Chl-a levels near the coast of the northern SCS. Their study area was adjacent to the mouth of the Mekong River, which discharges runoff that contains a high concentration of chromophoric dissolved organic matter (Shang et al., 2008). Two large phytoplankton blooms with high levels of Chl-a appeared in the SCS after typhoon Damrey (ID 200518), one in the open ocean and the other on the coast. The open-ocean bloom was caused by nutrient increases that resulted from mixing and upwelling, and the coastal bloom was caused by rainwater discharge. By these two mechanisms, both the wind and rain produced by typhoons can increase marine phytoplankton productivity (Zheng and Tang, 2007).

Near coasts, where nutrients are abundant, dense and often transient blooms of colonial centric diatoms develop. Biomass accumulates because diatoms outgrow their microbial competitors and macrozooplanktonic predators. Increased upward nutrient transportation after a typhoon's passage induces a bloom of chain-forming diatoms, because diatoms are capable of growing more rapidly than other phytoplankton under light-saturated and nutrient-replete conditions (Chai et al., 2007). In contrast, in the oligotrophic open ocean, small phytoplankton dominate. The grazers of small phytoplankton are also small, and have similar growth rates as their prey. Diatoms are the main contributors to the seasonal variability of biomass and primary productivity; small phytoplankton exhibit less seasonal variability (Ma et al., 2013).

In the model, phytoplankton functional groups consisted of small phytoplankton (s1) and diatoms (s2). Model simulations revealed that large phytoplankton are most responsive to typhoon-induced turbulent mixing and nutrient injection, with increases in biomass along the typhoon track. Small phytoplankton mainly move location and increase in spatial extent. On the coast, before the typhoon's arrival, s2 accounts for 50% of the total biomass; during the typhoon's passage and over the following several days, s1 comprises 90% of the total biomass. Approximately, two weeks after the typhoon has passed, s2 dominates again, and accounts for 60% of the total biomass.

5. Conclusions

We constructed a coupled three-dimensional physical-biogeochemical model (ROMS-CoSiNE) to evaluate the marine phytoplankton response to typhoon events in the SCS from 2000 to 2009. The model could reasonably reproduce the characteristics of the biogeochemical variables before and after typhoon passage. The results revealed that phytoplankton blooms were triggered after 43 typhoon events, and no significant blooms were found after 36 other typhoons. Of the 43 typhoon events that triggered blooms, 24 were in the open ocean and 19 were on the coast. Subsurface blooms were detected after five typhoon events that had no significant surface blooms.

In summary, we found the following:

- An increased nitrate concentration is the basic and key precondition for phytoplankton blooming in the oligotrophic SCS. In June, due to the deeper nutricline, even strong driving forces cannot uplift enough nitrate to the eutrophic zone, so few blooms are triggered.
- Typhoons can rapidly uplift nitrates from deep ocean layers, the concentrations of which gradually decrease after a typhoon's passage. Uplifted nitrates can trigger phytoplankton bloom, and Chl-a levels reach a peak 3 days later than nitrate levels.
- Typhoon intensity and translation speed both control the upward flux of nitrates. Slower translation speed induces strong wind stress and uplisfts more nutrients, means translation speed is more effective.
- Mesoscale eddies and the nutricline depth before a typhoon's arrival also affect bloom genesis.
- The mechanism involved in bloom formation on the coast is more complex than that in the open ocean, and phytoplankton functional groups also differ between the coast and the open ocean.

Acknowledgements

We thank Drs. Feng Nan, Peng Xiu, and Wentao Ma for their help with the ROMS-CoSINE model data retrieval and analysis. This work was financially supported by the National Natural Science Foundation of China (41430968, 41106105), the China-Sri Lanka Joint Center for Education & Research, Chinese Academy of Sciences, and the International Partnership Program of Chinese Academy of Sciences (131C11KYSB20160061).

References

Alexander, M., Capotondi, A., Miller, A., Chai, F., Brodeur, R., Deser, C., 2008. Decadal variability in the Northeast Pacific in a physical-ecosystem model: role of mixed layer depth and trophic interactions. J. Geophys. Res.: Oceans 113 (C02017).

Babin, S.M., Carton, J.A., Dickey, T.D., Wiggert, J.D., 2004. Satellite evidence of hurricane-induced phytoplankton blooms in an oceanic desert. J. Geophys. Res.: Oceans 109 (C03043).

Chai, F., Dugdale, R.C., Peng, T.H., Wilkerson, F.P., Barber, R.T., 2002. One-dimensional ecosystem model of the equatorial Pacific upwelling system. Part I: model development and silicon and nitrogen cycle. Deep Sea Res. Part II 49, 2713–2745.

Chai, F., Jiang, M.S., Chao, Y., Dugdale, R.C., Chavez, F., Barber, R.T., 2007. Modeling responses of diatom productivity and biogenic silica export to iron enrichment in the equatorial Pacific ocean. Glob. Biogeochem. Cycles 21 (GB3S90).
Chai, F., Liu, G., Xue, H., Shi, L., Chao, Y., Tseng, C.-M., Chou, W.-C., Liu, K.-K., 2009. Seasonal and interannual variability of carbon cycle in South China Sea: a three-dimensional physical-biogeochemical modeling study. J. Oceanogr. 65, 703–720.
Chen, Y.-L., Chen, H.-Y., Karl, D.M., Takahashi, M., 2004. Nitrogen modulates phytoplankton growth in spring in the South China Sea. Cont. Shelf Res. 24, 527–541.
Chen, Z., Hu, C., Muller-Karger, F., 2007. Monitoring turbidity in Tampa Bay using MODIS/Aqua 250-m imagery. Remote Sens. Environ. 109, 207–220.
Dugdale, R.C., Barber, R.T., Chai, F., Peng, T.H., Wilkerson, F.P., 2002. One-dimensional ecosystem model of the equatorial Pacific upwelling system. Part II: sensitivity analysis and comparison with JGOFS EqPac data. Deep Sea Res. Part II 49, 2747–2768.
Gierach, M.M., Subrahmanyam, B., 2008. Biophysical responses of the upper ocean to major Gulf of Mexico hurricanes in 2005. J. Geophys. Res.: Oceans 113 (C04029).
Gierach, M.M., Subrahmanyam, B., Thoppil, P.G., 2009. Physical and biological responses to Hurricane Katrina (2005) in a 1/25° nested gulf of Mexico HYCOM. J. Mar. Syst. 78, 168–179.
Gong, G.-C., Liu, K.K., Liu, C.-T., Pai, S.-C., 1992. The chemical hydrography of the South China Sea west of luzon and a comparison with the West Philippine Sea. Terr. Atmos. Oceanic Sci. 3, 587–602.
Hung, C.C., Gong, G.C., Chou, W.C., Chung, C.C., Lee, M.A., Chang, Y., Chen, H.Y., Huang, S.J., Yang, Y., Yang, W.R., Chung, W.C., Li, S.L., Laws, E., 2010. The effect of typhoon on particulate organic carbon flux in the southern East China Sea. Biogeosciences 7, 3007–3018.
Jaimes, B., Shay, L.K., 2009. Mixed layer cooling in mesoscale oceanic eddies during hurricanes Katrina and Rita. Mon. Weather Rev. 137, 4188–4207.
Kalnay, E., et al., 1996. The NCEP/NCAR 40-year reanalysis project. Bull. Am. Meteorol. Soc. 77, 437–471.
Lin, I., Liu, W.T., Wu, C.-C., Wong, G.T.F., Hu, C., Chen, Z., Liang, W.-D., Yang, Y., Liu, K.-K., 2003. New evidence for enhanced ocean primary production triggered by tropical cyclone. Geophys. Res. Lett. 30, 1718.
Lin, I.I., 2012. Typhoon-induced phytoplankton blooms and primary productivity increase in the western North Pacific subtropical ocean. J. Geophys. Res.: Oceans 117 (C03039).
Liu, G., Chai, F., 2009. Seasonal and interannual variability of primary and export production in the South China Sea: a three-dimensional physical–biogeochemical model study. ICES J. Mar. Sci.: J. du Conseil 66, 420–431.
Ma, W., Chai, F., Xiu, P., Xue, H., Tian, J., 2013. Modeling the long-term variability of phytoplankton functional groups and primary productivity in the South China Sea. J. Oceanogr. 69, 527–544.
Mendelsohn, R., Emanuel, K., Chonabayashi, S., Bakkensen, L., 2012. The impact of climate change on global tropical cyclone damage. Nat. Clim. Change 2, 205–209.
Morel, A., Huot, Y., Gentili, B., Werdell, P.J., Hooker, S.B., Franz, B.A., 2007. Examining the consistency of products derived from various ocean color sensors in open ocean (case 1) waters in the perspective of a multi-sensor approach. Remote Sens. Environ. 111, 69–88.
Naik, H., Naqvi, S.W.A., Suresh, T., Narvekar, P.V., 2008. Impact of a tropical cyclone on biogeochemistry of the central Arabian Sea. Glob. Biogeochem. Cycles 22, GB3020.
Parker, A.E., Wilkerson, F.P., Dugdale, R.C., Marchi, A.M., Hogue, V.E., Landry, M.R., Taylor, A.G., 2011. Spatial patterns of nitrogen uptake and phytoplankton in the equatorial upwelling zone (110°W–140°W) during 2004 and 2005. Deep Sea Res. Part II 58, 417–433.
Price, J.F., 1981. Upper ocean response to a hurricane. J. Phys. Oceanogr. 11, 153–175.
Shang, S., Li, L., Sun, F., Wu, J., Hu, C., Chen, D., Ning, X., Qiu, Y., Zhang, C., Shang, S., 2008. Changes of temperature and bio-optical properties in the South China Sea in response to Typhoon Lingling, 2001. Geophys. Res. Lett. 35 (L10602).
Shchepetkin, A.F., McWilliams, J.C., 2005. The regional ocean modeling system: a split-explicit, free-surface, topography following coordinates ocean model. Ocean Modell. 9, 347–404.
Shiah, F.-K., Chung, S.-W., Kao, S.-J., Gong, G.-C., Liu, K.-K., 2000. Biological and hydrographical responses to tropical cyclones (typhoons) in the continental shelf of the Taiwan Strait. Cont. Shelf Res. 20, 2029–2044.
Shibano, R., Yamanaka, Y., Okada, N., Chuda, T., Suzuki, S.-i., Niino, H., Toratani, M., 2011. Responses of marine ecosystem to typhoon passages in the western subtropical North Pacific. Geophys. Res. Lett. 38 (L18608).
Subrahmanyam, B., Rao, K.H., Srinivasa Rao, N., Murty, V.S.N., Sharp, R.J., 2002. Influence of a tropical cyclone on chlorophyll-a concentration in the Arabian Sea. Geophys. Res. Lett. 29, 2065.
Sun, L., Yang, Y., Xian, T., Lu, Z., Fu, Y., 2010. Strong enhancement of chlorophyll a concentration by a weak typhoon. Mar. Ecol. Prog. Ser. 404, 39–50.
Tang, D., Kawamura, H., Dien, T.V., Lee, M., 2004. Offshore phytoplankton biomass increase and its oceanographic causes in the South China Sea. Mar. Ecol. Prog. Ser. 268, 31–41.
Walker, N.D., Leben, R.R., Balasubramanian, S., 2005. Hurricane-forced upwelling and chlorophyll a enhancement within cold-core cyclones in the Gulf of Mexico. Geophys. Res. Lett. 32 (L18610).
Wang, X., Chao, Y., 2004. Simulated sea surface salinity variability in the tropical pacific. Geophys. Res. Lett. 31 (L02302).
Wang, G., Su, J., Ding, Y., Chen, D., 2007. Tropical cyclone genesis over the South China Sea. J. Mar. Syst. 68, 318–326.
Wang, S.-H., Hsu, N.C., Tsay, S.-C., Lin, N.-H., Sayer, A.M., Huang, S.-J., Lau, W.K.M., 2012. Can Asian dust trigger phytoplankton blooms in the oligotrophic northern South China Sea? Geophys. Res. Lett. 39 (L05811).
Wong, G.T.F., Ku, T.-L., Mulholland, M., Tseng, C.-M., Wang, D.-P., 2007. The SouthEast Asian Time-series Study (SEATS) and the biogeochemistry of the south China Sea—an overview. Deep Sea Res. Part II 54, 1434–1447.
Xiu, P., Chai, F., 2011. Modeled biogeochemical responses to mesoscale eddies in the South China Sea. J. Geophys. Res.: Oceans 116 (C10006).
Xiu, P., Chai, F., 2012. Spatial and temporal variability in phytoplankton carbon, chlorophyll, and nitrogen in the North Pacific. J. Geophys. Res.: Oceans 117 (C11023).
Xiu, P., Chai, F., Shi, L., Xue, H., Chao, Y., 2010. A census of eddy activities in the South China Sea during 1993–2007. J. Geophys. Res.: Oceans 115 (C03012).
Xiu, P., Chai, F., Xue, H., Shi, L., Chao, Y., 2012. Modeling the mesoscale eddy field in the Gulf of Alaska. Deep Sea Res. Part I 63, 102–117.
Xu, Y., Chai, F., Rose, K.A., Ñiquen, C.M., Chavez, F.P., 2013. Environmental influences on the interannual variation and spatial distribution of Peruvian anchovy (Engraulis ringens) population dynamics from 1991 to 2007: a three-dimensional modeling study. Ecol. Modell. 264, 64–82.
Ye, H.J., Sui, Y., Tang, D.L., Afanasyev, Y.D., 2013. A subsurface chlorophyll a bloom induced by typhoon in the South China Sea. J. Mar. Syst. 128, 138–145.
Zhang, S., Xie, L., Hou, Y., Zhao, H., Qi, Y., Yi, X., 2014. Tropical storm-induced turbulent mixing and chlorophyll-a enhancement in the continental shelf southeast of Hainan Island. J. Mar. Syst. 129, 405–414.
Zhao, H., Tang, D., Wang, Y., 2008. Comparison of phytoplankton blooms triggered by two typhoons with different intensities and translation speeds in the South China Sea. Mar. Ecol. Prog. Ser. 365, 57–65.
Zheng, G.M., Tang, D., 2007. Offshore and nearshore chlorophyll increases induced by typhoon winds and subsequent terrestrial rainwater runoff. Mar. Ecol. Prog. Ser. 333, 61–74.